Diagonalization of the Reynolds-averaged Navier–Stokes equations with the Reynolds-stress Turbulence Model

Patrik Rautaheimo and Timo Siikonen
Laboratory of Applied Thermodynamics
Antti Hellsten
Laboratory of Aerodynamics
Helsinki University of Technology, Espoo, Finland

1 Introduction

Because of the need for a general turbulence model that would work for arbitrary cases, the Reynolds-stress model (RSM) has gained popularity in turbulence modeling. Most RSM applications have been for incompressible flow. In that case Reynolds-stress forces act only in the momentum equations. Still, the coupling with the flow equations is a non-trivial task, see e.g. [1]. In the case of a compressible flow, Reynolds-stresses, as well as pressure, act not only in the momentum equations but also in the energy equation. This makes the implementation more complicated. Because the coupling between the Navier-Stokes equations and the Reynolds-stress equations is non-isotropic, time integration and upwinding are more complex than with algebraic or two-equation models.

In this study, Shima's low-Reynolds number RSM [2] is coupled with a compressible flow solver [3] based on Roe's method [4]. A new non-isotropic coupling method is introduced. The implicit solution method is modified in order to take account of the Reynolds stresses. The convergence is improved by using a multigrid acceleration. The model is applied for a channel flow and for a flow over an airfoil.

2 Governing Equations

The Reynolds-stress equations can be written in the following Cartesian tensor form

$$\rho \frac{D\widetilde{u_i'' u_j''}}{Dt} = P_{ij} + \Phi_{ij} - T_{ij} - \epsilon_{ij} - d_{ij} \tag{2.1}$$

where u_i'' is the Favre-averaged fluctuation velocity component in i-direction, tilde denotes Favre-averaging, and P_{ij}, Φ_{ij}, T_{ij}, ϵ_{ij} and d_{ij} are the production, the velocity pressure-gradient correlation, the turbulent transport, the dissipation rate and the diffusion terms, respectively. The turbulent transport, the velocity pressure-gradient and the dissipation rate must be modeled, whereas the production term is exact.

In this study Shima's model [2] is applied. Some modifications were needed in the velocity pressure-gradient term. The dissipation transport equation was taken from Chien's $k-\epsilon$ model [5] because it was found to be stable and well behaved. Shima's original equation was applied for the airfoil test case.

3 Numerical Method

Diagonalization of the flow equations

In the evaluation of the inviscid fluxes Roe's method [4] is applied. A rotation operator is used for the velocity components and also for the Reynolds-stresses. The flux is calculated as

$$\hat{F} = \mathcal{T}^{-1} F(\mathcal{T}U). \tag{3.2}$$

Here $\mathcal{T}$ is a rotation operator that transforms the dependent variables to a local coordinate system normal to the cell surface. In this way, only the Cartesian form F of the flux is needed. Velocity components are rotated from global to local coordinate system as

$$\begin{pmatrix} \hat{u} \\ \hat{v} \\ \hat{w} \end{pmatrix} = T \begin{pmatrix} u \\ v \\ w \end{pmatrix} \tag{3.3}$$

where the hats refer to the local Cartesian coordinate system. Matrix T is the rotation matrix that is determined by the normal and the tangent vectors of the cell face.

Correspondingly, the Reynolds-stresses are rotated from the global to the local coordinate system by the following formula

$$\hat{I} = T\, I\, T^T \tag{3.4}$$

where the components of the Matrix I are the Reynolds-stresses. Transformation from the local back to the global coordinate system is given by

$$I = T^T \hat{I} T. \tag{3.5}$$

The Cartesian form of the flux is

$$F(U^l, U^r) = \frac{1}{2}\left[F(U^l) + F(U^r)\right] - \frac{1}{2}\sum_{k=1}^{K} r^{(k)} |\lambda^{(k)}| \alpha^{(k)} \tag{3.6}$$

where U^l and U^r are the solution vectors evaluated on the left and right sides of the cell surface, $r^{(k)}$ is the right eigenvector of the Jacobian matrix $A = \partial F/\partial U$, the corresponding eigenvalue is $\lambda^{(k)}$, and $\alpha^{(k)}$ is the corresponding characteristic variable obtained from $R^{-1}\delta U$, where $\delta U = U^r - U^l$. A MUSCL-type approach has been adopted for the evaluation of U^l and U^r. In the evaluation of U^l and U^r, primary flow variables $V = (\bar{\rho}, \tilde{u}, \tilde{v}, \tilde{w}, \tilde{e})$, and conservative turbulent variables $(\bar{\rho}\widetilde{u_i'' u_j''}, \rho\epsilon)$ are utilized. Jacopian matrix A can be split in following ways

$$A = R\Lambda R^{-1} = M L \Lambda L^{-1} M^{-1} \tag{3.7}$$

where R and R^{-1} are the right and left eigenvector matrixes written by conservative variables, L and L^{-1} play the same role, with respect to the primitive variables, as the matrixes R and R^{-1}, Λ is the eigenvalue matrix, and M and M^{-1} are the transformation matrixes between the conservative and the primitive variables.

A coupling between the Navier–Stokes and the Reynolds-stress equations is introduced, since the Reynolds-stresses may be connected with the pressure [6]. In the i-momentum equation, the resulting effective pressure can be defined as

$$p_i^* = \bar{p} + \bar{\rho}\widetilde{u_i'' u_i''}. \tag{3.8}$$

In order to utilize Roe's method, the Jacobian of the flux vectors must be diagonalized. This requires that the Jacobian matrix of the flux vector has a complete set of eigenvectors. Unfortunately, linearly independent eigenvectors cannot be found if the non-isotropic pressure field of Eq.(3.8) is applied.

Since the non-isotropic pressure field is difficult to handle, the turbulent pressure is usually approximated by the mean of three components

$$p^* = \bar{p} + \frac{2}{3}\bar{\rho}k. \tag{3.9}$$

Using this, the flux vector can be divided into the isotropic and non-isotropic parts. The Jacobian of the isotropic part can be diagonalized. The effect of the non-isotropic part on a solution is small, and, consequently, it can be evaluated using central differences. In this approach, there is no need to rotate Reynolds-stresses in the local cell face coordinates. This diagonalization is similar to one of the $k - \epsilon$ model and can be found in [3].

The second method of diagonalization utilizes the production term P_{ij}. The production term is exact in RSM and it can be included into the vector F. This is not a conservative form of the vector F, but RSM is never in a strong conservative form because of the source terms.

The eigenvalues, i.e. the characteristic speeds of the combined matrix are

$$\begin{aligned} \lambda^{(i)} \quad = \quad & u, u + c, u - \sqrt{\widetilde{u'' u''}}, u - \sqrt{\widetilde{u'' u''}}, u + c, \\ & u, u + \sqrt{\widetilde{u'' u''}}, u + \sqrt{\widetilde{u'' u''}}, u, u, u, u \end{aligned} \tag{3.10}$$

where c is the speed of sound. For an arbitrary equation of state, the speed of sound is

$$c^2 = p_e\, p/\rho^2 + p_\rho + 3\widetilde{u'' u''}. \tag{3.11}$$

Using the primitive variables, the characteristic variables are

$$\delta W = L^{-1}\delta V = R^{-1}\delta U \tag{3.12}$$

where $\delta V = V^r - V^l$. The left eigenvector matrix L^{-1} and right eigenvector matrix R are relatively complicated and can be found in [7].

In matrix L^{-1} and R there are terms that have to be limited to avoid unnatural behaviour between turbulent and unturbulent regions. For example, the term $\widetilde{u''v''}/\sqrt{\widetilde{u''u''}}$ or $\delta(\widetilde{u''v''})/\sqrt{\widetilde{u''u''}}$ must not get very large values when $\widetilde{u''u''}$ goes to zero. It can be shown that

$$\sqrt{\widetilde{u''u''}}\sqrt{\widetilde{v''v''}} \geq |\widetilde{u''v''}|. \tag{3.13}$$

Using this $\widetilde{u''v''}/\sqrt{\widetilde{u''u''}}$ can be limited as

$$\frac{|\widetilde{u''v''}|}{\sqrt{\widetilde{u''u''}}} \leq \sqrt{\widetilde{v''v''}}. \tag{3.14}$$

Time Integration Method

In the implicit stage the approximate factorization is done assuming isotropic Reynolds-stresses. The algorithm consists of a backward and forward sweep in every coordinate direction. The sweeps are based on a first-order upwind differencing. In addition, the linearization of the source term is factored out of the spatial sweeps.

The matrix inversion resulting from the source-term linearization is performed before the spatial sweeps. The matrix D is approximated by using the following pseudo-linearization

$$D = \frac{\partial Q}{\partial U} = -\frac{Q}{|\Delta U_{\max}|}. \tag{3.15}$$

In this way, the maximum change of U caused by Q is limited to $|\Delta U_{\max}|$. The value of $|\Delta U_{\max}|$ is evaluated as in [3].

A multigrid method is used to accelerate the convergence. In order to stabilize the multigrid cycle with Reynolds stresses, several devices have been developed. The implementation for the multigrid cycling is described in [3].

4 Test Calculations

Channel Flow

The model was checked by calculating a fully developed flow in a plane channel. Several methods were compared. The numbering of the test cases can be seen in Table 1. The second-order upwind scheme was used. The results were compared with those of Kim et al. [8] DNS data and the Reynolds-stress budgets were compared with Mansour et al. [9] data. The DNS data is at $Re_m = \rho u_m \delta/\mu \approx 2800$, where u_m, δ and μ are the mean velocity, the channel half-width and molecular viscosity, respectively. Because a compressible flow solver is used, the Mach number was set to 0.2. This introduced a 1% change in density across the channel. Calculations were performed with five multigrid

Table 1 Description of the test cases.

Case 1	Isotropic flux difference splitting with diffusion of Daly et al. [10]
Case 2	Non-isotropic flux difference splitting with diffusion of Daly et al.
Case 3	Non-isotropic flux difference splitting with the scalar diffusion [11]
Case 4	Same as case 2 with a single grid

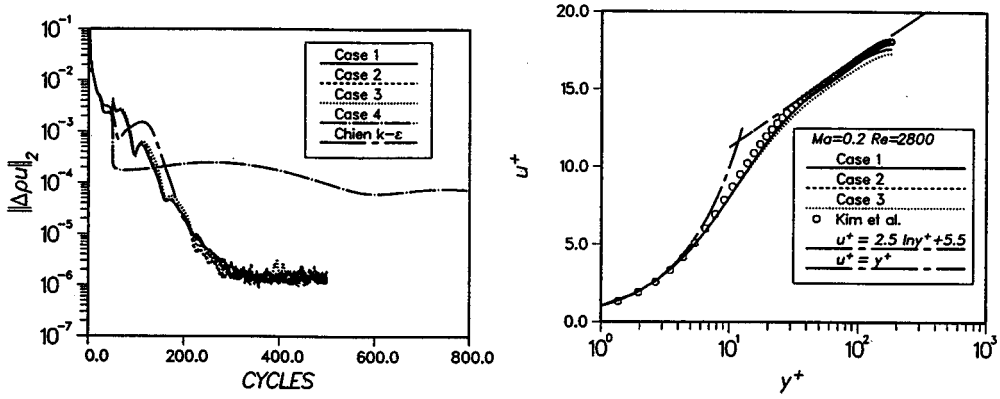

Figure 1 Convergence of the L_2-norm of the x-momentum residual and mean velocity profiles in wall coordinates.

Table 2 Mean flow variables.

	DNS	Case 1	Case 2	Case 3
δ^*/δ	0.141	0.135	0.133	0.135
θ/δ	0.087	0.081	0.080	0.082
$H = \delta^*/\theta$	1.62	1.66	1.67	1.64
$c_f = \tau_w/(\frac{1}{2}\rho u_m^2)$	8.18×10^{-3}	8.45×10^{-3}	8.43×10^{-3}	8.72×10^{-3}
$Re_\tau = \rho u_\tau \delta/\mu$	180	181	181	184
$Re_m = \rho u_m = \delta/\mu$	2800	2817	2819	2819
$Re_c = \rho u_c \delta/\mu$	3250	3256	3252	3259
u_m/u_τ	15.63	15.55	15.62	15.36

levels at $CFL = 10$. The first 50 iteration cycles were performed with a $k-\epsilon$ model and the Reynolds-stresses were not coupled with flow equations. A converged solution was obtained after 350 iteration cycles.

The convergence history of the L_2-norm of the x-momentum is shown in Fig. 1. In this case also the difference in the convergence rate between the isotropic, non-isotropic methods and $k-\epsilon$ model is marginal, whereas the effect of the multigrid acceleration is significant. However, two times higher CFL numbers could be used with the $k-\epsilon$ model.

Mean flow variables are presented in Table 2. As can be seen in Table 2, the difference between isotropic and the non-isotropic flux difference splitting was small. The velocity

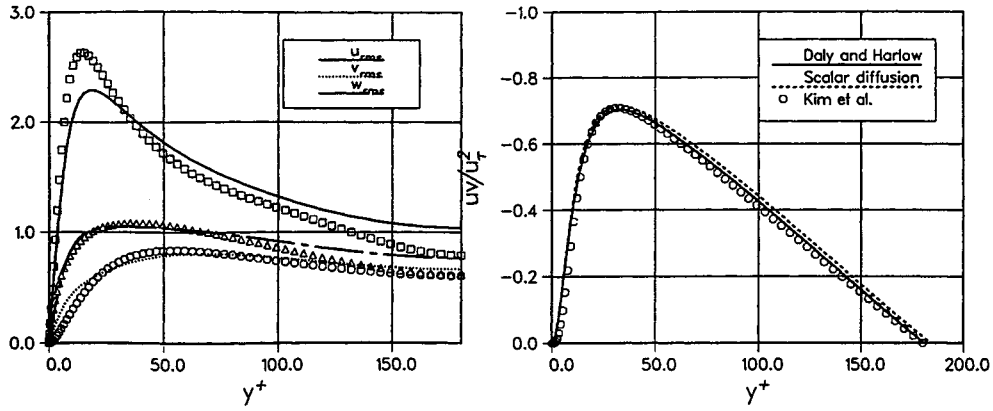

Figure 2 Comparision of the calculated Reynolds-stresses and the DNS-data in the plane channel.

profiles are also compared in Fig. 1. Velocity profiles in the viscous sublayer agree well with the DNS data and the universal profile. On the outer layer the velocity profiles are not completely satisfactory. The Reynolds-stresses can be seen in Fig.2, where $u_{rms} = \sqrt{\widetilde{u''u''}/u_\tau^2}$. Turbulent intensities agree well with the DNS data, except that u_{rms} peak level is low and the near wall values v_{rms} are not satisfactory. Shear-stress in Fig. 2 agrees with DNS.

Onera A-airfoil

For this case the experimental data was provided by Capbern et al. [12] and Gleyzes [13]. The Reynolds number and the Mach number are 2.1×10^6 and 0.15, respectively. The angle of attack is 13.3 degrees. The RSM is compared with the two-equation model of Chien and the Cebeci-Smith algebraic turbulence model. The dissipation equation is the same as in Shima's original article [2]. More detail can be found in [14]. In this case only the isotropic flux splitting method was used. Skin friction coefficient and pressure coefficient distributions can be found in Fig. 3.

5 Summary

The Reynolds-averaged Navier–Stokes equations with a low-Reynolds number RSM have been solved using an implicit method with a multigrid acceleration for convergence. In the evaluation of fluxes Roe's method is applied and the turbulence equations are coupled with the inviscid part of the flow equations. A new non-isotropic coupling of the Navier–Stokes and the Reynolds-stress equations was introduced.

This paper has focused attention on the problem of coupling the Reynolds-stresses with Navier–Stokes equation in a compressible case. The main conclusion is that when

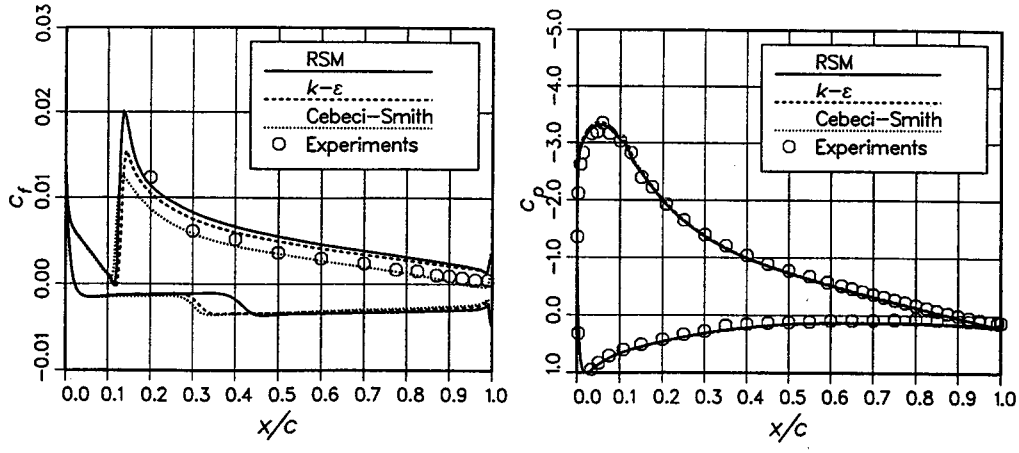

Figure 3 Skin friction coefficient and pressure coefficient distributions around the Onera A-airfoil.

Roe's flux-difference splitting is applied, the Reynolds stress equations can be coupled with Navier-Stokes equations if the effect of the production term is included in the Jacobian matrix. The resulting eigenvectors and the characteristic variables have a fairly complex form. In the present examples the new coupling method had only a minor effect on the results and on the convergence rate. However, with a computational approach this form can be rearranged and simplified. As a result the computing time is increased by only 13% in comparison with the non-isotropic coupling. The iteration sweep in RSM was roughly 2.5 times slower than in Chien's $k - \epsilon$ model.

References

[1] F.S. Lien and M.A. Leschziner. A general non-orthogonal collocated finite volume algorithm for turbulent flow at all speeds incorporating second-moment turbulence-transport closure, part 1: Computational implementation. *Computer Methods in Applied Mechanics and Engineering*, pages 123–148, 1994.

[2] N. Shima. A Reynolds-stress model for near-wall and low-Reynolds-number regions. *Journal of Fluids Engineering*, 110:38–44, 1988.

[3] T. Siikonen. An application of Roe's flux difference splitting for the $k-\epsilon$ turbulence model. Report, Series A A-15, Helsinki University of Technology, Laboratory of Aerodynamics, 1994. ISBN 951–22–2059–8.

[4] P.L. Roe. Approximate Riemann solvers, parameter vectors, and difference schemes. *Journal of Computational Physics*, 43:357–372, 1981.

[5] K. Chien. Predictions of channel and boundary-layer flows with a low-Reynods-number turbulence model. *AIAA Journal*, 20(1):33–38, Jan 1982.

[6] D. Vandromme. Turbulence modeling for turbulent flows and implementation in Navier–Stokes solvers. In *Introduction to the Modeling of Turbulence*. von Karman Institute for Fluid Dynamics Lecture Series 1991-02, 1991.

[7] P.P. Rautaheimo and T. Siikonen. Numerical methods for coupling the Reynolds-averaged Navier–Stokes equations with the Reynolds-stress turbulence model. Report 81, Helsinki University of Technology, Laboratory of Applied Thermodymics, 1995. ISBN 951–22–2748–7.

[8] J. Kim, P. Moin, and R. Moser. Turbulence statistics in fully developed channel flow at low Reynolds number. *Journal of Fluid Mechanics*, 177:133–166, 1987.

[9] N.N. Mansour, J. Kim, and P. Moin. Reynolds-stress and dissipation-rate budgets in a turbulent channel flow. *Journal of Fluid Mechanics*, 194:15–44, 1988.

[10] B.J. Daly and F.H. Harlow. Transport equations of turbulence. *Physics of Fluids*, 13:2634–2649, 1970.

[11] L. Davidson. Prediction of the flow around an airfoil using a Reynolds stress transport model. *Journal of Fluids Engineering*, 117:50–57, March 1995.

[12] C. Capbern and C. Bonnet. Operation decrochage. Rapport final de synthese. Technical Report 443.535./89, Report Aerospatiale, Toulouse, 1989.

[13] C. Gleyzes. Operation decrochage. resultats de la deuxieme campagne d'essais a f2- (mesures de presion et velocimetrie laser). CERT 57/5004.22- OA 72/2259 AYD, ONERA, 1989.

[14] A. Hellsten. Reynold-stress model in computational aerodynamics (in Finnish). Master's thesis, Helsinki University of Technology, May 1995.